# Spatial & Spectral Variation of Seaways


S. Barrett[1], I. Ashton[2], T. Lewis[1], and G. Smith[2]

[1]Hydraulics & Maritime Research Centre,
University College Cork,
Ireland
E-mail: `hmrc@ucc.ie`

[2]PRIMaRE,
University of Exeter,
United Kingdom,
E-mail: `I.G.C.Ashton@exeter.ac.uk`



## Abstract

The wave energy industry is entering a new phase of pre-commercial and commercial deployments of full-scale devices, so better understanding of seaway variability is critical to the successful operation of devices. The response of Wave Energy Converters (WEC) to incident waves govern their operational performance and for many devices, this is highly dependant on spectral shape due to their resonant properties. Resource assessments, device performance predictions and monitoring of operational devices will often be based on summary statistics and assume a standard spectral shape such as Pierson-Moskowitz or JONSWAP. Furthermore, these are typically derived from the closest available wave data, frequently separated from the site on scales in the order of 1km. Therefore, variability of seaways from standard spectral shapes and spatial inconsistency between the measurement point and the device site will cause inaccuracies in the performance assessment. Potential differences in estimated and actual incident wave power are investigated using measured data. Concurrent wave data from two wavebuoys have been collected from the EMEC full scale test facility in Orkney, Scotland and the Galway Bay benign test site, Ireland along with single buoy data from the Wave Hub site off the north Cornwall coast in the UK.

Spatial variability is investigated through the examination of limited data from wave measurements taken at separations of 200m, 500m and 1500m. Differences between concurrent measurements are identified and compared to theoretically predicted variability, in terms of their magnitude and statistical properties. Comparisons of the data over the available separations indicate a possible dependence of the measured differences in the spatial domain, although site-specific properties must also be considered.

The deviation of the measured data from the empirically derived spectral shapes is investigated, quantified and compared to other sites from published data. This investigation involves the identification of bi-modal seaways and it is found that this deviation reduces with increasing wave height, although the degree of deviation, which is being investigated here, is site specific to some degree.

Finally, this analysis is implemented for chosen elements of the wave height-period scatter diagram that are populated at the selected sites. The analysis techniques derived are employed to quantify not only spatial and spectral variation and variability, but also variations from benign site to full-scale site. The analysis highlights potential variations in power incident at a site from those estimated using a standard spectral shape at a separate measurement point.

The results of the work presented here are only indicative as the spectral variation work is based on just four months of data, while the spatial variation exercise is applied to just 1 month's concurrent measurements. Robust conclusions can only be drawn when the methods are applied to a more extensive database.





**Keywords:** wave energy, wave spectra, bootstrap analysis,


## Nomenclature

| | | |
|---|---|---|
| $H_s$ | = | Significant wave height, derived either in the time or frequency domain |
| $H_{m0}$ | = | Significant wave height, derived from spectral estimates |
| $T_z$ | = | Zero-crossing wave period |
| $T_p$ | = | Peak wave period |
| $DH_i$ | = | Percentage difference in $i^{th}$ concurrent measurements of significant wave height, $H_{m0}$ |
| $DH^*_b$ | = | $b^{th}$ bootstrap iteration of $DH_{i:N}$ |
| $\theta_b$ | = | The mean of the $b^{th}$ iteration, $DH^*_b$ |
| $N$ | = | Total number of $H_{m0}$ values in each data set |
| $B$ | = | Number of iterations used in bootstrap |
| $\lambda$ | = | Deep water wavelength |
| $m_p$ | = | The $p^{th}$ spectral moment |
| $f$ | = | Frequency |
| $f_u$ | = | The upper frequency cut-off used in estimation of the wave spectrum |
| $P$ | = | Wave power per metre crest length |
| $\rho$ | = | density of water, 1025 kg/m$^3$ |
| $g$ | = | acceleration due to gravity, 9.81 m/s$^2$ |
| $\lambda_F$ | = | Froude scale parameter |

### Subscripts

| | | |
|---|---|---|
| $i$ | = | record number, $i = 1,\ldots,N$ |
| $b$ | = | bootstrap iteration number, $b = 1,\ldots,B$ |
| $p$ | = | Number of spectral moment |

### Superscripts

| | | |
|---|---|---|
| * | = | Bootstrap iteration |

# 1 Introduction

Direct measurements from a wave energy site provide a data set of the wave field incident on the devices. Prior to deployment, this data is applied to resource assessments and device performance predictions [1], and during operation, for monitoring of device response and performance [2]. The placement of wave sensors around a development will be outside of the immediate proximity of the devices, where they cannot interfere with normal device operation and radiated or reflected waves from the devices do not interfere with measurements. In the protocols for performance assessments of WECs, a minimum separation of 100 metres and a maximum of 1km are proposed [3]. In order to transpose measurements from the measurement site to the devices, it is necessary to quantify any differences in the wave field at the two points. A detailed investigation of the site, including bathymetry or tidal regimes can reveal possible deterministic factors that will affect the wave-field. Such an investigation coupled with modelling sensitivity studies are also advised [3].

These sensitivity studies can be undertaken in the spatial domain and in the frequency domain. Site specific conditions can influence the energy distribution of a spectrum, especially in areas where locally generated wind seas, due to fetch limited conditions coexist with the remnants of far distant storms that seep into the investigation area as swell. For wave energy extraction knowledge of the sea state spectral components is essential both for power extraction calculations and control issues as this information can be hidden within the historical summary statistics.

# 2 Spatial Variation

The irregularity of ocean waves causes an inherent variability in the sea surface profile. It follows that any measurements made of the sea surface will also reflect this variability. Goda used simulation tests to demonstrate an increase of variability between wave measurements with the distance between them [4]. Identifying deterministic differences in wave measurements requires differentiation between random variability and the deterministic differences under examination. As variability increases with the distance between sites, it can serve to mask deterministic differences, making them more difficult to quantify. Furthermore, variability will also have a direct effect on the determination of the short term performance of WECs.

Three wave data sets were used for the spatial analysis, each consisting of one month of data taken by two concurrently operating wavebuoys. The wavebuoys are separated by a different distance for each data set, 200m at the Galway Bay benign test site, Ireland, and 500m and 1500m at the EMEC full scale test facility in Orkney, Scotland. An effort has been made to select data that exhibit the maximum cross-over in the wave states measured. The two data sets from the EMEC test site have similar H-T scatter diagrams. However, the wave climate at Galway Bay means that the wave states here are generally smaller in terms of both H and T. In order to reduce the dependence of results on the properties of the incident wave states, the variability in wave measurements across these distances are characterised using the percentage difference in concurrent $H_{m0}$ values determined from 30 minute records of the surface profile. The bootstrap method is a statistical technique which involves the re-sampling of the available data [5]. Here, it is applied to the percentage differences in concurrent $H_{m0}$ values to estimate the probability distribution of the mean difference. In doing so, it takes into account the variability in the measured data to define what levels of mean difference can be considered significant. The analysis highlights some of the difficulties inherent in measuring spatial variations in wave fields.

## 2.1 Methods

### *2.1.1 Spatial Differences*

The differences between spectrally derived significant wave height values, $H_{m0}$, from spatially separated wave records were analysed using three data sets, where concurrent measurements were available for a period of 1 month (Table 1).

To ensure data sets are comparable, they were converted to parameters derived from 30 minute averages. Datawell Waverider buoys derive their spectral parameters from an average of 16 segments taken during a 30 minute period. In this analysis, only 30 minute periods where at least 14 of the 16 segments are available from both buoys are included in the analysis, thus ensuring high integrity, concurrent data. Visual checks and examination of the source data removed further errors. These processes limit the amount of data available for each of the three sites and the available data is shown in Table 1.

Once the concurrent data sets were identified for each thirty minute record, the differences in concurrent data from buoy A and B, *DH*, were calculated as the percentage difference in the value of $H_{m0}$. Thus for $i = (1,2,3\ldots, N)$

$$\mathrm{DH_i} = \frac{\mathrm{H_{m0}}(\mathrm{A_i}) - \mathrm{H_{m0}}(\mathrm{B_i})}{\frac{1}{2}\left[\mathrm{H_{m0}}(\mathrm{A_i}) + \mathrm{H_{m0}}(\mathrm{B_i})\right]} \times 100 \qquad (1)$$

where $H_{m0}(A_i)$ is the significant wave height value calculated for 30 minute record *i*, at buoy A, and $\frac{1}{2}\left[H_{m0}(A_i) + H_{m0}(B_i)\right]$ is the average value of $H_{m0}$ for the record, *i*. Figure 1 shows a time series of *DH* for a period of three days. Mean and standard deviations of *DH* were calculated. The probability distribution of *DH* values were estimated using the relative frequency of occurrence of differences in 100 bins of 1% between -50% and +50% (Fig. 2).

| Data set (site and date) | Separation (m) | Available data (no. of 30 min records) | Available data (days) |
|---|---|---|---|
| EMEC 07/2004 | 1500 | 1481 | 30days 20hrs |
| EMEC 09/2006 | 500 | 1268 | 26days 10hrs |
| Galway 06/2008 | 200 | 1213 | 25days  6hrs 30mins |

**Table 1.** Data sets used, and the available data for the three sites after processing.

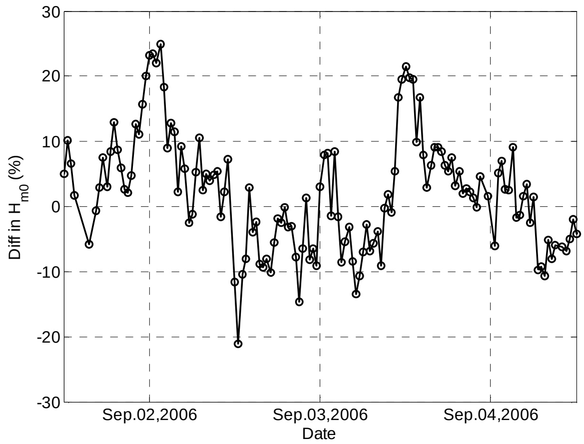


**Figure 1.** An example of time-series of percentage differences between concurrent $H_{m0}$ values across a separation of 500m for a three day period.

| Site | Separation | Differences (%) | |
|---|---|---|---|
| | | Mean | Std Dev |
| EMEC A and B | 1500m | -0.28 | 10.94 |
| EMEC B and C | 500m | 1.07 | 7.32 |
| Galway 1 and 2 | 200m | 2.98 | 4.81 |
| Goda | 5λ | 0.0043 | 7.42 |

**Table 2.** Mean and standard deviation of the differences between concurrent measurements of $H_{m0}$.

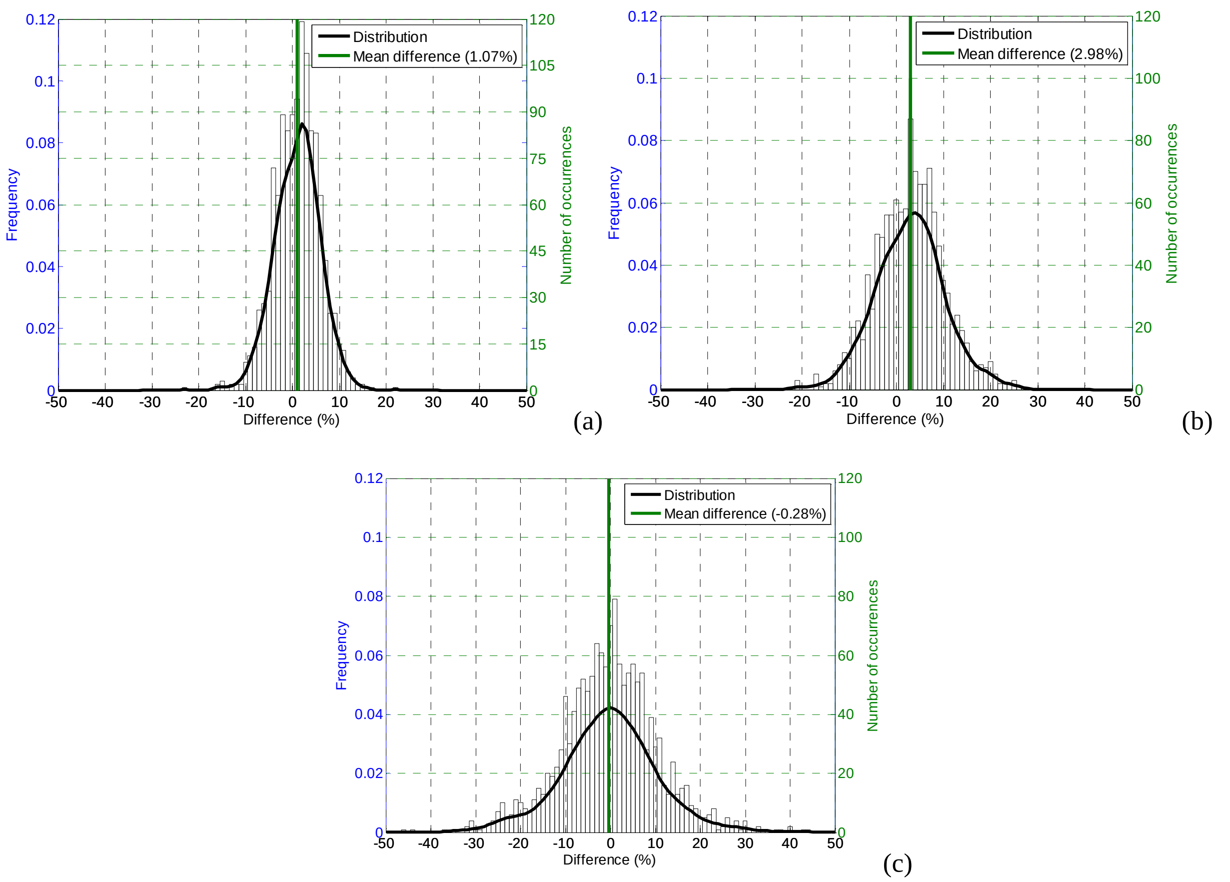


**Figure** 2. The frequency distribution (left hand y axis) superimposed onto a histogram (right hand y axis) of differences between concurrent Hm0 values, both calculated over 100 bins of width 1%. Also shown is the mean difference. (a) 200m separation at Galway Bay, (b) 500m separation at the EMEC site, and (c) 1500m separation at the EMEC site.

### 2.1.2 Bootstrap for Significance of Differences

Bootstrapping is a statistical technique that derives an empirical distribution function (EDF) of a statistical parameter of a dataset in order to estimate the true distribution of that parameter. It avoids parametric assumptions as the EDF is calculated from the original sample [5]. Here, the bootstrap was applied to the dataset of differences between concurrent $H_{m0}$ values, *DH*, comprising N values. For each bootstrap iteration, *N* sample values from the dataset *DH* were drawn at random, with replacement, giving a new set of data, $DH^*_b$ of equal length to the original dataset. This was repeated for *B* iterations and the mean value was found for each. For *b = (1,2,3…B)*

$$\theta_b = \mu(DH^*_b) \qquad (2)$$

giving *B* values of $\theta_b$, where $\mu(DH^*_b)$ is the mean of the $b^{th}$ iteration, $DH^*_b$. Subsequently, the distribution of $\theta$ can be estimated, which represents the EDF of the mean difference. The value of *B* used in this analysis was 100. In order to determine if there was a significant difference between the data sets, 95% confidence intervals were calculated by determining the range within which 95% of $\theta_b$ lie. Where these limits did not encompass a mean difference of 0, this indicated that there was a residual difference between the two buoys at the site.

## 2.2 Results

### 2.2.1 Mean Differences

The estimated distribution of $\theta$, calculated using bootstrap analysis for each data set are shown in Fig. 3. The 5% and 95% confidence limits of these distributions demonstrate that the mean difference between concurrent measurements of $H_{m0}$ can be considered significant for the separation of 200m at Galway Bay and the separation of 500m at the EMEC site (Figs. 3a & 3b). However, from the data with a spatial separation of 1500m at the EMEC site, the difference in mean $H_{m0}$ measured between buoys A and B is not considered significant because the estimated distribution encompasses zero within the confidence limits.

### 2.2.2 Variability

The variability in the differences for each site can be categorised by their distributions (Fig. 2). For each data set, the differences can be seen to approximate a normal distribution, which is in accord with that expected due to random variability. However, it does not rule out the presence of periodic deterministic differences. The standard deviations of the percentage differences between concurrent $H_{m0}$ values are used to demonstrate the variability in the measurements (Table 2). The standard deviation of the differences is observed to increase with the distance of separation between the buoys (Fig. 4). Putting these values in context, a measure of $H_{m0}$ taken 1500m from a device, at a 95% confidence can be expected to vary by up to 20%. When the separation is reduced to 200m, this value is reduced to 10% (Table 2).

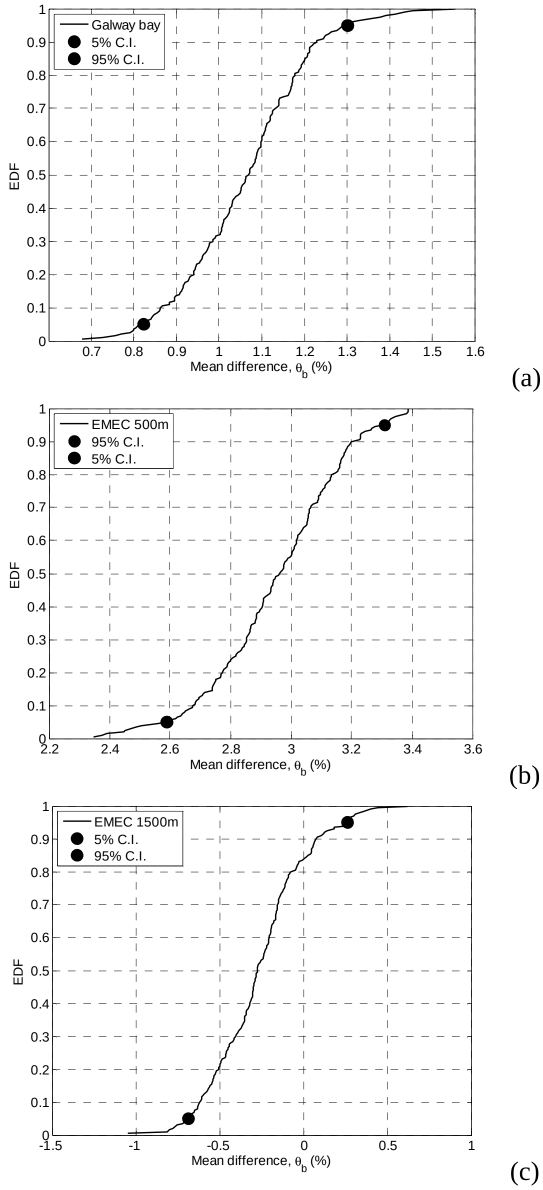


**Figure 3.** Results of the bootstrap analysis for (a) Galway Bay, (b) EMEC, 500m and (c) EMEC, 1500m, showing the empirical distribution function of the mean differences. Also shown are the confidence limits calculated as 5% and 95% of the bootstrap means, $\theta_b$.

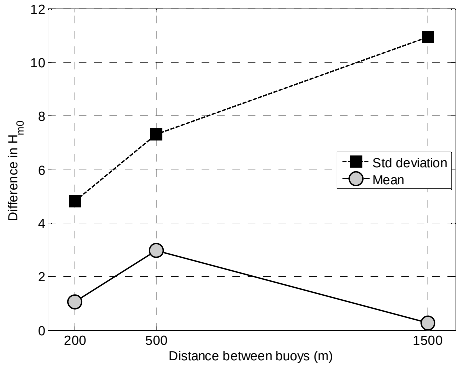


**Figure 4.** The magnitude of the mean and the standard deviations of the differences in $H_{m0}$ for each separation.

### 2.2.3 *Comparison with Simulation Tests*

Goda used simulated surface profiles to examine the effect of spatial separation on the variability of estimations of the significant wave height [4]. A record length of 100 waves is used and spatial separation is defined in terms of the wavelength as 5λ, where λ is the deep water wavelength [7].

$$\lambda = \frac{g}{2\pi} T_p^2 \text{ [m]} \tag{3}$$

When comparing these values to the measured data, there are two factors to be considered which will affect the variability.

Firstly, the record lengths used in the measured data equate to more than 100 waves therefore, variability would be expected to be lower than in the simulations. Secondly, when expressed as a function of λ, separation will show a dependency on the wave state, which varies in the measured data. Accordingly, a direct comparison of measured results with the results in [4] has not been attempted in this paper. However, using the average peak wave period at each site, 5λ can be estimated for the measured data sets (Table 3).

| Site | Actual separation (m) | Mean $T_p$ (s) | λ (m) | Equivalent separation, 5λ (m) |
|---|---|---|---|---|
| EMEC A and B | 1500 | 8.76 | 119.20 | 595.80 |
| EMEC B and C | 500 | 10.20 | 158.60 | 793.18 |
| Galway Bay 1 and 2 | 200 | 6.66 | 69.25 | 346.24 |

**Table 3.** The equivalent separation of simulation tests by Goda [1977] calculated from the measured average peak wave period for each data set.

For the EMEC data from buoys A and B, the average measured peak period defines a wavelength, λ of 119.2m and therefore a 5λ separation of 595.8m which is significantly less than the 1500m separation in the measured data (Table 3). Thus, the measured data would be expected to exhibit higher variability. For the remaining two data sets, the measured data would be expected to have a lower variability than the simulation tests. This prediction is in agreement with the results from the measured data, where only the EMEC A and B data set (σ = 10.94) is seen to exceed the σ predicted in simulation tests (σ = 7.42) (Table 2). These provisional results would have to be confirmed using a more detailed simulation to allow direct, quantitative comparisons.

## 3 Spectral Variation

Having dealt with wave variability in the spatial domain, it is also important to consider the deviations of the spectral shape in the frequency domain. For the purpose of this analysis a limited data from the Galway Bay and Wavehub test sites are considered and compared. From the outset it is important to note that conclusions drawn from this analysis is based on a limited data set from the Wavehub location. This data set covered a period from December 2005 to April 2006. Therefore, it is proposed that further investigation should be carried out when a more extensive data set is available from the test site to endorse the findings of this section of the paper. Due to this confined period of data availability from the Wavehub site, the same time period will be investigated for the Galway Bay test site. Both data sets were recorded by Datawell Waverider buoys which utilise the same methodology to measure waves.

### 3.1 Summary Statistics

The historical measurement of a seaway are the hourly summary statistics that have been derived either spectrally or temporally (or both) usually from the vertical heave of the buoy. However, it is becoming apparent that this outline of the characteristics of the sea state does not relay the required level of information for wave energy device developers. All the knowledge that is required can be derived from the spectrum, although even the method of acquiring this is subject to discussion [6].

To accurately calculate the efficiency of a WEC, the incident power of the sea state has to be determined and the most common method of achieving this is by using the summary statistics typically in the following approximation:

$$P = 0.55 H_s^2 T_z \text{ [kW/m]} \tag{4}$$

However, this equation is based on empirically derived spectral distributions. Wave power is originally derived from the relationship between power and energy as described in [7] and Equation 5 below where the dependence is on the spectral moment, $m_{-1}$:

$$P = \frac{\rho g^2}{4\pi} m_{-1} \text{ [W/m]} \tag{5}$$

This method of wave power calculation (Eqn. 5) utilises the spectral moment, which is a fundamental element of the spectrum, rather than the summary statistics, therefore the incident wave power calculated using this method should be more indicative of the variability of the spectral shape. The variation of spectral shape for similar summary statistics has been shown in a previous paper [8]. The deviation of the spectral shape from the expected empirical fit will also change the relationship of wave height and period in the power equation. Another assumption is subject to the upper and lower frequency limits of the spectrum, but in the case of the two data sets used here, the limits are approximately the same. The spectral generation techniques of the data sets are different, therefore the associated errors of the spectral estimates will be different. The assumption is that this does not greatly influence the results, although it is something that requires investigation. The frequency details of the two data sets are given in Table 4.

Figure 5 shows a regression of the incident wave power from both the Wavehub and Galway Bay test sites for the winter period from December 2005 until

April 2006. Although Equation 5 has units of Watts per metre wave crest, it is generally converted to kilowatts per metre. The incident power, calculated using the spectral moment, is plotted along the abscissa while the wave power determined from the summary statistics is plotted against the ordinate axis. The disparity between the incident wave power calculated from both methods is in the region of 10-15% for the data set used for this analysis. This may indicate that due to the non-conformity of the spectral shape to empirically derived distributions such as Pierson-Moskowitz or JONSWAP, the estimate of the incident wave power at a WEC when using the summary statistics alone can be underestimated by as much as 15% in all sea states.

| Data Set | Min Freq [Hz] | Max Freq [Hz] | Frequency Step [Hz] |
|---|---|---|---|
| Galway Bay | 0.03 | 0.665 | 0.005(0.03-0.665) |
| Wavehub | 0.025 | 0.58 | 0.05(0.025-0.095)<br>0.01(0.1-0.58) |

**Table 4**. Spectral frequency information.

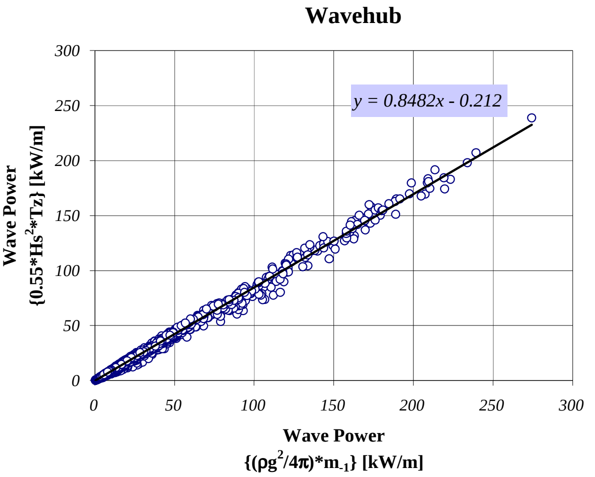


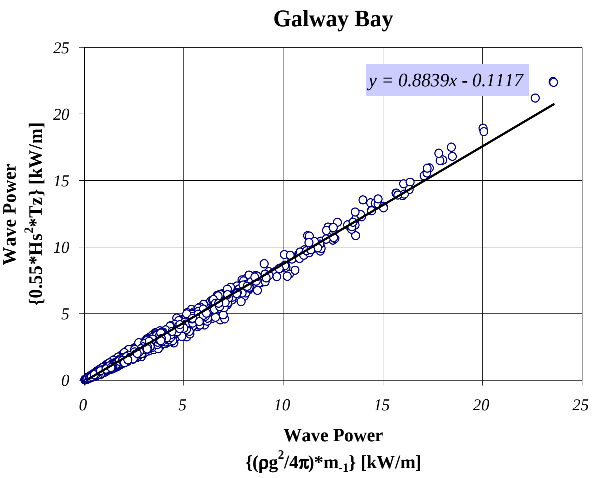


**Figure 5**. Regression plot of Power Calculation Method for Galway Bay and Wavehub Test Sites.

### 3.2 Bimodal Sea States

Another important indicator of spectral variation is the occurrence of bimodal sea states. A thorough investigation of the spectral shapes of these measured sea states was conducted to quantify the existence of double peaked spectra. The findings of similar investigations reported in literature for both open ocean and coastal sites in the North Atlantic have found various degrees of influence of twin peaked spectra. Guedes Soares reports that an overall average of 22% of bimodal spectra occur in the North Atlantic [9]. This is averaged across all occurring wave heights and ranged from 34% at low significant wave heights (1-2m) to 3.4% with $H_s$ greater than 10m. Later work [10], which dealt with an even greater catalogue of data, including data from the North Sea, confirmed the findings of the previous paper [9] and stated an average of 16% double peaked spectra occurrence for the North Sea, again for all wave heights that occurred. Other authors have found similar percentage occurrences for other areas of the North Atlantic, as documented in Table 5. Again, the evidence of these studies, the work presented in [11] and this paper support the findings that the percentage occurrence decreases as the significant wave height increases by Guedes Soares [10].

| Author | Year | Location | Average % Occurrence |
|---|---|---|---|
| Cummings [12] | 1981 | North Atlantic | 25% |
| Guedes Soares [9] | 1984 | North Atlantic | 22% |
| Aranavachapun [13] | 1987 | North Atlantic | 24% |
| Guedes Soares [10] | 1991 | North Sea | 16% |
| Guedes Soares [14] | 1992 | Portugal Atlantic | 23-26% |

**Table 5**. Reported Double Peaked Average Percentage Occurrence from Literature.

To quantify the influence of bimodal sea states at a site of interest, the spectral shape is required for inspection, as the energy distribution is lost within the summary statistics. Various methods exist for the identification of bimodal spectra and are readily found in the literature for application to both directional and non-directional spectral data. The method adopted in this study is applied to non-directional spectra and is based on identifying legitimate peaks of energy in the spectrum, not just variations due to sampling errors. The identification procedure applies the following guidelines to classify legitimate peaks in the spectra:

i. A peak is classified as legitimate if the centre ordinate in a frequency range of ±0.05Hz is the maximum in that range.
ii. Secondary peaks qualify as such if the secondary peak magnitude is greater than 15% of the magnitude of the primary peak.
iii. A peak is discounted if it is within 2 seconds of an identified peak larger in magnitude.

This identification methodology is applied to both data sets from the Wavehub and Galway Bay test sites. The Wavehub data set was limited to four months from December 2005 to March 2006. Due to this limited set of data, the Galway Bay data chosen for the analysis was also limited to the same time frame for comparison. The multi-peak identification procedure results in an overall average percentage occurrence of approximately 15% of all the spectra exhibiting bimodal features at the Galway Bay data set. This compares to 8% for the Wavehub test site. The higher percentage of double peaked spectra at the Galway Bay site is largely due to its location within a semi-enclosed bay on the west coast of Ireland. At this site, fetch limited local wind seas exist in parallel with an encroaching offshore swell that diffracts around islands to the west of the site which shelter the bay from the Atlantic. The long period swell that occurs at the Wavehub site may be from the open Atlantic Ocean to the west. An analysis of the directional components of the individual peaks will identify if there is a pattern or source to their formation, although this is outside the scope of this paper.

The percentage of bimodal seas that occur, distributed over a range of wave heights, and for all periods, is shown in Figure 6 for the two test sites. At the Wavehub site, 7.41% of all spectra that occur have a significant wave height less than 1m. Just over 5% of these are identified as being double peaked. For the wave height range of 1m $\leq H_s <$ 2m, 47.28% of spectra occur, with over 20% of these being classified as double peaked spectra. In Galway Bay 71.17% of spectra have a significant wave height less than 1m although over 40% are bimodal. For the range with $H_s$ between 1m and 2m at the benign site, 26.54% occur, 12.48% of which are twin peaked.

Focusing on the $H_s$ range of 1-2m, the distribution of the proportion of bimodal sea states against wave period can be investigated, as shown in Figure 7. This shows that in the case of the Wavehub test site, which for the wave height range of 1m to 2m selected has occurrence in average periods from 3s to 12s (see Figure 8), the majority of the double peaked spectra occur at an average period of the overall spectrum of 4s to 5s. In fact, double peaked spectra at the Wavehub site, where the overall significant wave height ranges from 1m to 2m, only occur in the period range of 3s to 7s, comparable to the Galway Bay site, which shows a similar characteristic.

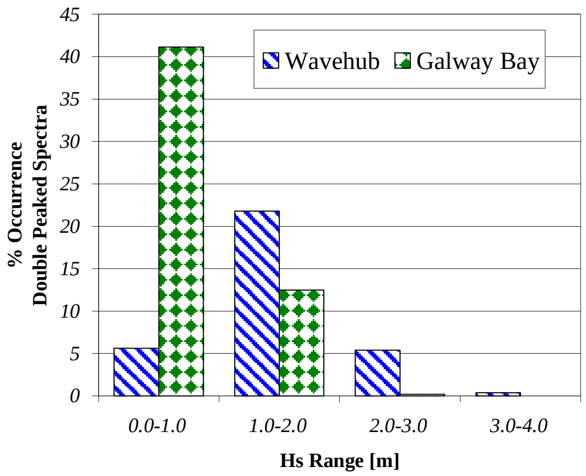


**Figure 6**. Distribution of the percentage occurrence of bimodal seas for all wave periods at the Wavehub and Galway Bay sites.

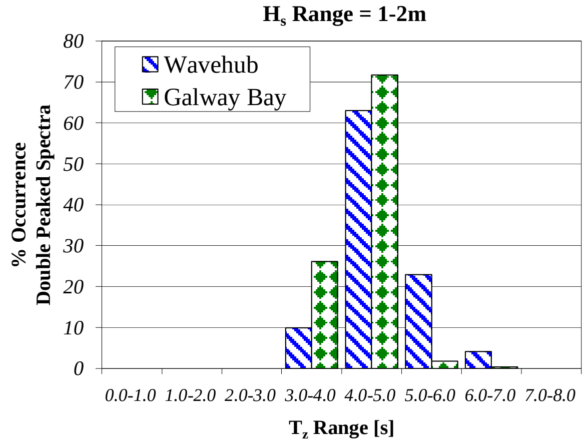


**Figure 7**. Distribution of the percentage occurrence of bimodal seas only in the range $H_s$=1-2m, for all wave periods at the Wavehub and Galway Bay sites.

It should be noted however that these figures may change when a more thorough data set is analysed due to the occurrence of a greater number of low wave height sea states during the Summer months, which would increase disproportionately the number of twin peaked spectra.

### 3.3 Bi-variate Scatter Summary

The bi-variate scatter diagram is employed to ascertain an overall picture of the conditions at a test site. This quickly indicates the percentage of extremes of the sea states that have been experienced at the site but also the most likely sea state that has occurred during the period of data collection. The knowledge gained can then be combined with a similar plot containing the efficiency or power potential of a device, to establish the production value of that WEC at a particular site.

Both the Wavehub and Galway Bay test sites have quite different characteristics, as can be seen from the area covered by the bi-variate scatter in Figure 8. This is expected of a benign test site and a commercial demonstration zone. In fact, it would appear that on the basis of these scatter plots, the Galway Bay test site is at a scale of $\lambda_F$ = 1:2 with respect to the Wavehub site. However, as previously stated, the caveat with this assumption is that it is based on a limited data set of only four months. A much greater data set is required to produce a statistically qualified scatter diagram.

A scatter diagram element with a significant wave height, 1m $\leq H_s <$ 2m and zero-crossing period, 4s $\leq T_z$ < 5s was chosen as it is common to both the Wavehub and Galway Bay site and marked by a circle in Figure 8 is selected for further investigation. This selected element has a percentage occurrence for the Galway Bay and Wavehub site of 17.45% and 19.09%, respectively which is approximately 350 spectra for the winter period for both sets of data. This element was chosen to show that for the same summary statistics, two wave deployment sites can have different characteristic spectral shapes. Figure 9 shows the individual spectra that occurred within this single scatter element at both sites during the duration of the data set for Galway Bay and Wavehub respectively. The average of the spectral ordinates and the equivalent classical shaped Bretschneider spectra are also plotted against frequency. The summary statistics of the Bretschneider spectrum are the equivalent mid-points of the scatter diagram element, in this case $H_s$ = 1.5m and $T_z$ = 4.5s. Reference to Figure 7 shows over 60% of the Galway Bay spectra and 70% of the Wavehub spectra are double peaked for this selected scatter diagram element of $1\text{m} \leq H_s < 2\text{m}$ and $4\text{s} \leq T_z < 5\text{s}$.

The averaged spectra of each site for this combination of summary statistics are very different to each other and the classical shape of the equivalent Bretschneider spectrum. The Wavehub averaged spectrum has a distinctive twin peak while the Galway Bay average spectrum appears very broad. This indicates that there is little variation of the wind and swell generation systems at the Wavehub site, which may be further explained by investigation of the directional spectrum. It would then be easier to predict the peak periods of the wind and swell seas. This may be explained by the less complicated bathymetry at the more exposed Wavehub test site in comparison to the confined Galway Bay site. It is not clear from Figure 9 that any double peaked seas exist at the Galway Bay site, however the bar chart of Figure 7 indicates that a high proportion of these spectra are in fact bimodal. Therefore the wide shape of the average spectrum shown in Figure 9 for Galway Bay may indicate a large temporal variation in the bimodal spectral shape at this site for this bi-variate scatter element. It would be easy to assume that a WEC being excited in these conditions at both sites would produce significantly different power levels, an aspect that would require further investigation by the device development teams.

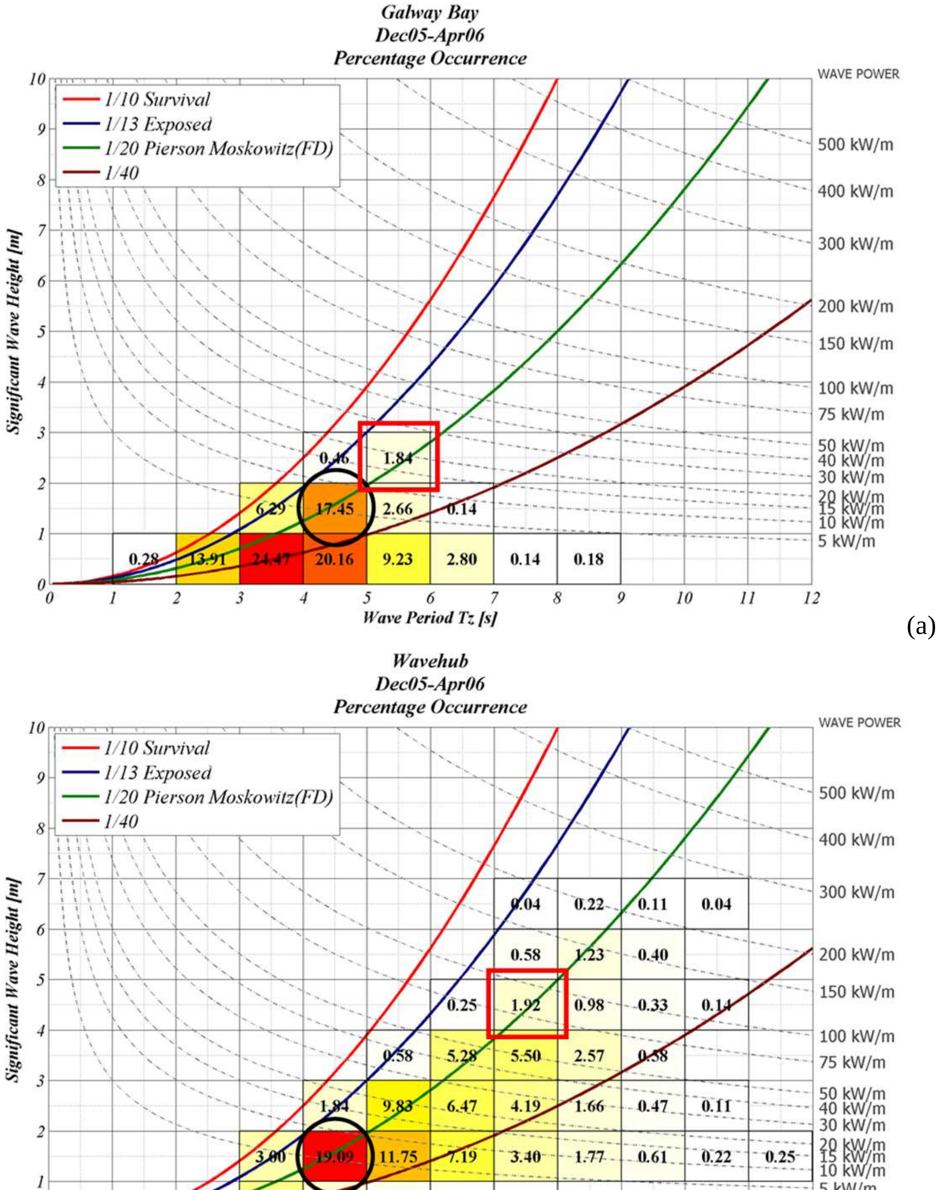


**Figure 8**. Bi-variate Scatter Plot of $H_s$-$T_z$ for the (a) Wavehub and (b) Galway Bay test sites respectively.

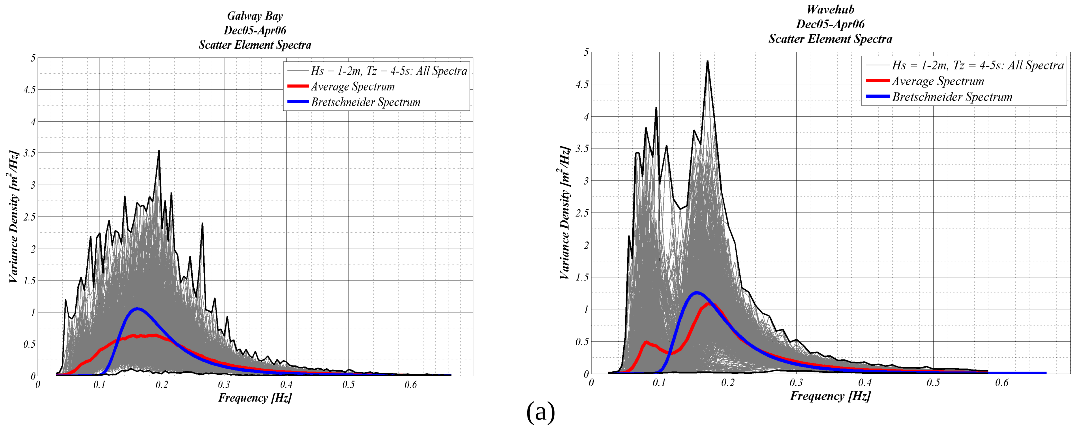


(a) (b)

**Figure 9**. Individual, averaged and classical spectra within the selected scatter element, $H_s$: 1-2m and $T_z$: 4-5s, as circled in Figure 8, for (a) Galway Bay (17.45%) and (b) Wavehub (19.09%) test sites respectively.

Having selected a component of the scatter diagram common to both sets of data, an element indicative of extreme sea states was chosen individually for each site. In this study of extremes however, the Galway Bay extreme element has only a quarter of the wave power of the Wavehub test site element and so they are not directly comparable. However, as the Galway bay site appears to be a half scale of the Wave Hub location, these two scatter diagram elements are compatible by Froude scaling. The study does show the reduction in bimodal spectral characteristics at both sites in these extreme cases. The different elements of the scatter diagram for each site that were chosen are indicated in Figure 8 by the outlined squares. This allows the conformity of the average spectral shape to classical spectra in storm type sea states to be investigated. The two different scatter elements were chosen as they both have similar spectral occurrences and fall on the fully developed line, therefore having the same significant steepness.

From the Wavehub scatter diagram of Figure 8, an element with $H_s$ between 4-5m and $T_z$ of 7-8s was chosen. This represented 1.92% of all spectra in the data set, which totals approximately 50 spectra. The Galway Bay test site does not experience seas of this magnitude, so a lower element was selected with a $H_s$ of 2-3m and $T_z$ of 5-6s. The extreme scatter element chosen for Galway Bay represents 1.84% or approximately 40 spectra of that data set. Figure 10 shows the selected storm sea bi-variate elements. The Bretschneider spectrum in both plots of Figure 10 was dictated by the median significant wave height and average period of the respective scatter diagram element. Note that the ordinate scales are not the same for both plots of Figure 10.

The average spectra for each of these higher wave height scatter diagram elements no longer exhibit bimodal properties, although again there are significant differences to the equivalent Bretschneider spectra. These differences in the variance density from what is expected at each site may have a large influence on the power production of a WEC, especially if the resonant frequency coincides with the maximum ordinates shown in Figure 10.

## 4 Conclusion

In this paper, the differences between concurrent values of significant wave height, $H_{m0}$, measured by wavebuoys separated over three different distances have been examined. In order to test whether these differences can be attributed to random variability, their mean values were tested using bootstrap methods. That they can be considered significant for two of the three site locations indicates the influence of site-specific deterministic effects. These could be due to physical factors affecting the waves, such as the tidal regime or the bathymetry, or residual differences in the wave sensors, however the causes have not been examined here.

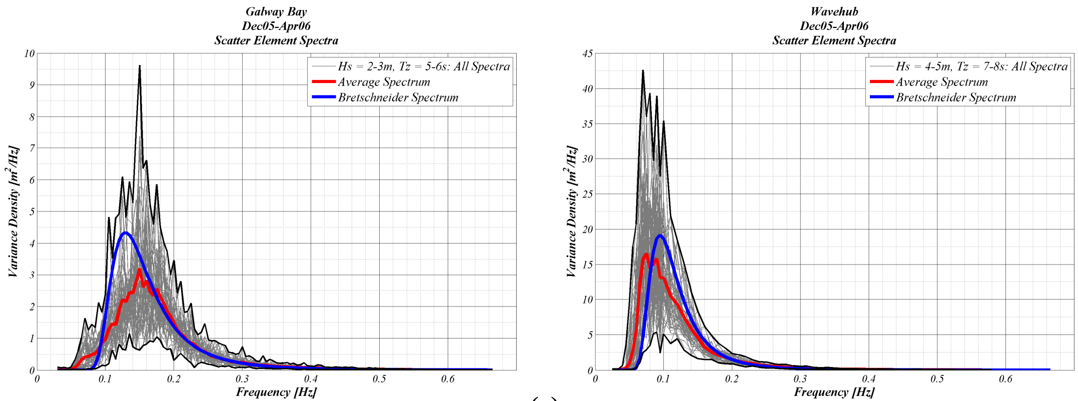


(a) (b)

**Figure 10**. All Spectra of Scatter Element $H_s$: 2-3m and $T_z$: 5-6s for Galway Bay (a) and Scatter Element $H_s$: 4-5m and $T_z$: 7-8s for Wavehub (b) Test Sites Respectively.

The width of the confidence intervals derived for the mean difference using this technique demonstrates the effect of variability inherent in wave measurements on the investigation of differences between wave data sets. A more variable data set leads to wider confidence intervals and a reduction in sensitivity of the analysis.

The differences follow a normal distribution, and demonstrate an increase in variability with distance separation. For measurements between two spatially separated wave sensors, the inherent random variability encountered increases with the distance between the measurement points. This effect is predicted by simulation tests, which support the measured data [4]. However, a direct comparison between the simulations and the measured data was not possible. This could be achieved by repeating the simulation to more realistically model the measurement cases.

When assessing the characteristics of a potential deployment site, it is important to not only investigate the summary statistics but also the distribution of variance of the spectral shape. The variability of the spectral shape was investigated in a number of ways. From measurement to measurement within a chosen location, across the scatter diagram and comparison between sites, and it was found that site specific conditions can have a large influence in the expected spectral shape and its conformity to empirically derived spectral distributions. The influence this will have on the power production of WECs will not be known until such time as they are deployed at sea or modelled effectively.

For short term measurements, the observed increase in variability will increase uncertainty in power estimations for a site and mask deterministic differences in the wave record. Where long-term data sets are employed to investigate deterministic factors, an increase in variability will increase the amount of data required to separate variability from deterministic differences. Therefore, when transposing measurements across a site, or measuring the difference in the wave field between two (or more) points, the increased variability associated with the spatial separation and spectral shape must be taken into account.

It was also shown that both the Wavehub site and the Galway Bay test zone confirm the findings of previous studies by Guedes Soares and others. For both test sites, the number of double peaked spectra declined as the wave height increased, indicating that this is an issue only in low sea states to varying degrees and dependant on site characteristics.

In order to further quantify the results of the spectral variation analysis, it is recommended that this work is extended with a larger data set incorporating directional measurements at both the Galway Bay and Wavehub sites. Further work should consider dependence of variability on the spectrum of the incident waves, and the influence of deterministic differences.

## Acknowledgements

The authors would like to acknowledge, with grateful thanks, John Lawrence (EMEC), Helen Smith (PRIMaRE), and Caitriona Nic Aonghusa (Marine Institute) for providing the data that was used from the respective wave energy test sites; EMEC, Wavehub and Galway Bay.

## References

[1] Halcrow. Wave Hub coastal processes study report, Halcrow and the South West Regional Development Agency, published online www.wavehub.co.uk, 2006.

[2] EMEC. Performance Assessment for wave energy conversion systems in open sea test facilities. The European Marine Energy Test Centre Report. Published on-line www.emec.org.uk/downloads.asp, 2004

[3] DTI. Preliminary device performance protocol, version 1.3. March 2007.

[4] Goda. Y. Numerical experiments on statistical variability of ocean waves. *Report of the port and harbour research institute*, Vol. 16 (2), June 1977

[5] B.Efron and R.J.Tibrishani. *An introduction to the bootstrap.* Chapman and Hall, 1993.

[6] G. Rodriguez, C. Guedes Soares and U. Machado. Uncertainty of the sea state parameters resulting from the methods of spectral estimation. *Ocean Engineering*, V.26, No.10, 1999.

[7] M.J.Tucker and E.G.Pitt. *Waves in ocean engineering* Elsevier ocean engineering book series Vol.5. Elsevier, 2001.

[8] S.Barrett, B. Holmes and T. Lewis. Monitoring of Seaway Variability on WEC Performance. *2nd Int. Conference in Ocean Engineering*, Brest, 2008.

[9] C. Guedes Soares. Representation of Double-Peaked Sea Wave Spectra. *Ocean Engineering*, V.11, No.2, 1984.

[10] C. Guedes Soares. On the Occurrence of Double Peaked Wave Spectra. *Ocean Engineering*, V.18, No.1/2, 1991.

[11] S.Barrett, B. Holmes and T. Lewis. Scalability of a Benign Wave Energy Test Site. *In Proc. 7th European Wave & Tidal Energy Conference*, Porto, 2007.

[12] W.E. Cummings, S.L. Bale and D.M. Gentille. Hindcast waves for engineering applications. *Proc. Int. Sym. on Hydrodynamics in Ocean Engineering*. Trondheim, 1981.

[13] S. Aranuvachapum. Parameteres of JONSWAP spectral model for surface gravity waves-II. Predictability from real data. *Ocean Engineering*. V.14, No.2, 1987

[14] C. Guedes Soares and M.C. Nolasco. Spectral modelling of sea states with multiple wave systems. *J. Offshore Mechanics and Arctic Engineering*. V.114, No.4, 1992.